



UNIVERSITY
OF WOLLONGONG
AUSTRALIA

University of Wollongong
Research Online

Faculty of Engineering - Papers (Archive)

Faculty of Engineering and Information Sciences

2000

Droplet Size Regulation in the Short Circuit GMAW Process using a Controlled Current Waveform

Dominic Cuiuri

University of Wollongong, dominic@uow.edu.au

John Norrish

University of Wollongong, johnn@uow.edu.au

Christopher David Cook

University of Wollongong, chris_cook@uow.edu.au

<http://ro.uow.edu.au/engpapers/1329>

Publication Details

Cuiuri, D, Norrish, J & Cook, CD, Droplet Size Regulation in the Short Circuit GMAW Process using a Controlled Current Waveform, Proceedings Gas Metal Arc Welding for the 21st Century, 2000, p 173-185, USA: American Welding Society.

Research Online is the open access institutional repository for the University of Wollongong. For further information contact the UOW Library:
research-pubs@uow.edu.au

DROPLET SIZE REGULATION IN THE SHORT CIRCUIT GMAW PROCESS USING A CONTROLLED CURRENT WAVEFORM

D. Cuiuri^{*}, J. Norrish^{*}, C.D. Cook[#]

ABSTRACT

Enhanced control of the short-circuit gas metal arc welding (GMAW) process can be achieved through the use of an advanced power source applying a controlled current waveform. By using a current waveform whose period is adapted to suit the requirements of the process, excellent welding performance can be achieved. When the current waveform is of fixed peak amplitude and shape, the control can be considered to be open-loop, as there is no active attempt to regulate a specific process parameter such as arc length, fusion area or dipping frequency. There is scope for more sophisticated control of the process. Using a typical open loop control strategy as a benchmark, an alternative closed loop control is evaluated here. The technique regulates the size of the droplet formed on the end of the electrode on a cycle-by-cycle basis. The instantaneous melting rate is modelled in a real-time welding controller, and the current waveform is adapted to achieve the desired droplet size, as determined from the time integral of the instantaneous melting rate.

KEYWORDS

Short circuit GMAW, Current waveform control, droplet size.

INTRODUCTION

The concept of using a controlled current waveform in the short circuit GMAW process has been developed since the mid 1960s to overcome inherent limitations of the constant voltage power source. Smith (Ref. 1) used a duplex power source in 1966 to overcome lack-of-fusion defects in pipe welding. The current delivered during the arcing period was supplied independently of the current required for metal transfer and rupture in the short circuit period. In 1972 to 1974, Boughton and MacGregor (Refs. 2,3) produced a transistorised power source which could produce a programmable current waveform which was regulated so that spatter was significantly reduced and process stability was dramatically improved. These goals were achieved by imposing a reduced-current "wetting-in" period at the start of the short circuit to reduce repulsion forces, and by reducing the short circuiting current immediately prior to rupture of the short-circuit bridge to eliminate violent bridge rupture. However, the technology existing at that time did not allow for product commercialisation. The main problems were high cost and an inability to predict the onset of short-circuit rupture at changing CTWDs (contact tip to workpiece distances). In 1987, Ogasawara et al (Refs 4,5) reported commercial application of a power source based on the same principles as those applied by Boughton and MacGregor, but utilising

* Faculty of Engineering, University of Wollongong, Australia

Faculty of Informatics, University of Wollongong, Australia

the benefit of a decade of significant advances in electrical engineering technology. A major improvement was the ability to detect the onset of a short circuit rupture for varying CTWDs. The waveforms are shown in Figure 1. In 1993, Stava (Ref.6) reported a further commercial development of this concept, incorporating a transistor switch in the output circuit to significantly reduce short-circuit current turnoff time, and an improved means of predicting the onset of short-circuit rupture by using dV/dt measurement. The waveforms reported by Stava, shown in Figure 2, show that a similar approach has been taken to that of Ogasawara et al.

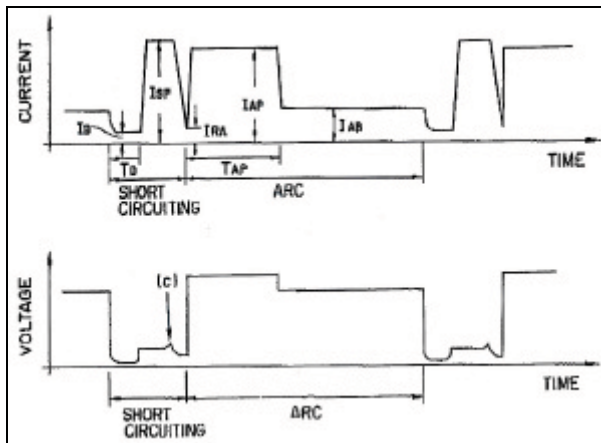


Figure 1 Waveforms from (Ref. 5)

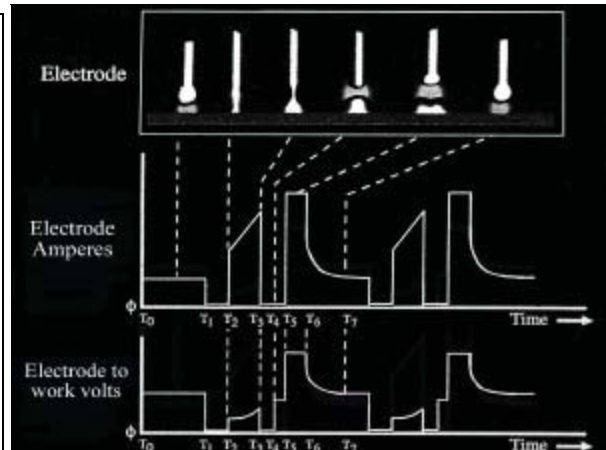


Figure 2 Waveforms from (Ref.6)

These improvements in short-circuit welding power source technology were a result of a continually improving understanding of the GMAW process. The developments of Boughton and MacGregor followed from a fundamental assessment of the short-circuiting process (Ref. 7). At around the same time, Kiyohara et al (Ref 8) proposed that the stability of the short-circuit process and spatter generation mechanisms could be explained by analysing the mechanisms responsible for transfer of material from the droplet formed on the end of the electrode to the weld pool on the workpiece. In particular, analysis showed that successful and stable metal transfer from electrode to workpiece requires that the droplet is above a certain size. More specifically, the length of the metal bridge L_b formed between the solid electrode and the weld pool must be longer than a critical value L_b^* , as shown in Figure 3. The critical length is a complex function of electrode diameter and the short circuit current. It was also deduced that if the bridge length is above a certain value L_d , then metal transfer would occur without the assistance of current. The corollary to these findings is that the current applied to the process during the arcing period must not only provide adequate workpiece melting, but must also produce an adequately sized droplet at the electrode tip, to ensure stable operation. The calculation of electrode melting rates in open-arc GMAW have been empirically investigated since the 1950s (Ref.9). A rigorous fundamental approach was taken by Halmoy (Refs 10-12), who demonstrated that the instantaneous melting rate can be calculated if the relationship between resistivity and heat input for the electrode material is known:

$$v(t) = \frac{\phi \cdot i(t)}{A(H_m - H_L(t))} \quad (\text{Eq. 1})$$

where $v(t)$ is the instantaneous melting rate, $i(t)$ is the instantaneous current, ϕ is the work function of the electrode material, A is the electrode cross-sectional area, and H_m is the energy per unit volume (J/mm^3) required to melt the electrode material and raise the temperature of the molten droplet to the final value before being transferred to the weld pool. H_m is assumed to be constant. $H_L(t)$ is the increase in specific heat content (J/mm^3) of an element of electrode which has been generated by resistance heating as it travels from the contact tip to the end of the electrode through a distance L . The distance L is the stickout length, and is approximately equal to the CTWD during the short circuiting period. The term $H_L(t)$ is calculated by evaluating the action integral $W(t)$ in equation 2, and using the relationship in Figure 4 to determine the corresponding value of H_L . The relationship between H_L and W is found experimentally by heating a length of electrode wire and instantaneously measuring energy input and resistance. Figure 4 is reproduced from Halmoy (Refs 10-12), showing H_L vs W for common materials.

$$W(t) = \int_{-\tau}^0 j^2(t) dt = \frac{1}{A^2} \int_{-\tau}^0 i^2(t) dt \quad (\text{Eq. 2})$$

In equation 2, τ is the transit time, required for an element of electrode to travel from the contact tip to the tip of the electrode. It is a function of the CTWD and wire feed speed. The practical implementation of this electrode melting rate model is discussed in the next section.

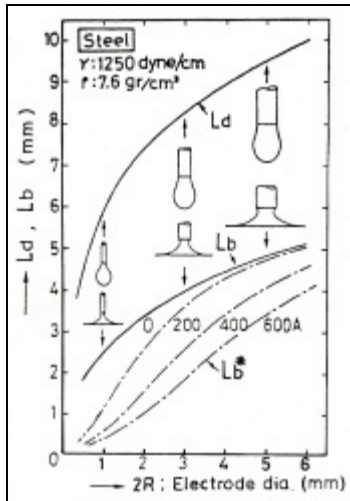


Figure 3 Critical droplet length (Ref. 8)

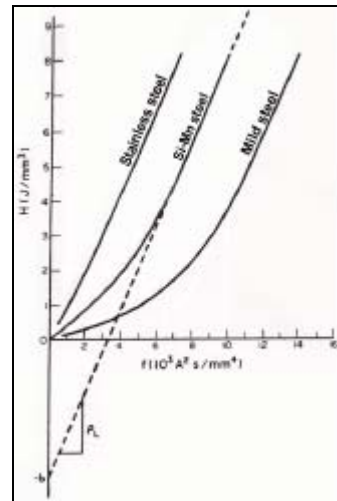


Figure 4 H_L versus W (Ref. 12)

As a final aspect of research into the short-circuit GMAW process, an objective and quantitative measure of the stability of the process has been developed by a number of researchers (Refs 13-15). The calculation of *stability indices* is performed to evaluate the consistency or repeatability of the process. These indices are based on the periodicity of the welding cycle. The measure of stability used in this paper is described by equation 3:

$$\text{Stability Index} = 1 - \frac{\sigma}{\mu} \quad (\text{Eq. 3})$$

where σ is the standard deviation of the weld cycle duration, and μ is the mean value of the weld cycle. A perfectly regular process will achieve a stability index of 1.0, whilst a very unstable weld will yield a figure between 0.0 and approximately 0.3.

The following sections describe the practical implementation of the melting rate model in a real time controller which operates a sophisticated current-controlled power source. In closed loop operation, the current is reduced to a low value towards the end of the arcing period, when the target droplet size is achieved. There are two objectives of droplet size regulation. Firstly, it is expected that process regularity, hence stability index, would be improved due to the higher uniformity of metal transfer to the weld pool. Secondly, decreased spatter levels are expected since the initial short circuiting current is lower than for the open loop case. The performance of the closed loop process is evaluated, and compared against that of the open loop process, which is used as the benchmark.

TEST EQUIPMENT AND METHOD

A specialised power source designed specifically for the short-circuiting process was constructed, having all of the features of the commercial power sources described in the previous section. It is controlled from a PC-based DSP (digital signal processor) controller, which is readily programmable in a high level language. References and logging data are transferred between PC and DSP through a common memory area. The interrupt-based controlling rate is set to 25kHz (40 μ s). Custom signal conditioning and isolating equipment was also constructed to interface the power source to the controller. The welding torch is fixed above a moving table, to which workpiece samples are clamped. The welding travel speed is regulated by a small AC variable speed drive. The fixed torch arrangement allows for either still photography or high speed filming of the welding process.

Two versions of controlling software were developed. The first version provides the type of process control described by Stava (Ref. 6) and Ogasawara et al (Ref. 5). Typical current and voltage waveforms are shown in Figure 5. All of the indicated parameters are regulated by the controller/power source except for the duration of states 3, 4 and 1, which are determined by the voltage events within the process itself. This type of control is described as "open loop". Although the control inherently adapts to the time requirements of the process, there is no active closed loop regulation of a specific process parameter such as arc length or heat input.

The second version of software proposes to improve process regularity, hence stability, by regulating the size of the droplet formed on the tip of the electrode. When the estimated droplet size reaches the target value, the arcing current is reduced to a low background level of 20A. This is sufficient to provide a pilot arc for short-circuit detection, and produces a minimum of additional droplet growth. The current is ramped from I_{arc_min} rather than being rapidly terminated, so that excitation of additional weld pool oscillations is avoided. Because the short-circuits occur at very low arcing current, spatter due to ball repulsion at the weld pool is expected to be minimal. The closed loop waveforms are illustrated in Figure 6.

Welding tests were conducted using 0.9mm mild steel electrode to AWS ER70S-6 specification, with Ar-23%CO₂ and CO₂ shielding gases. The behaviour of the open loop process was investigated at a wire feed speed of 1.9 to 5.7 m/min, at CTWDs from 8mm to 20mm. The tests consisted of bead-on-plate trials using 5mm descaled MS plate. The key assessment parameters were stability index, fusion area, and spatter level. The region of best performance was

determined from the combination of these parameters, and the closed loop process was then tested in the same operating region. The two sets of results were then compared, to evaluate the improvement in process performance.

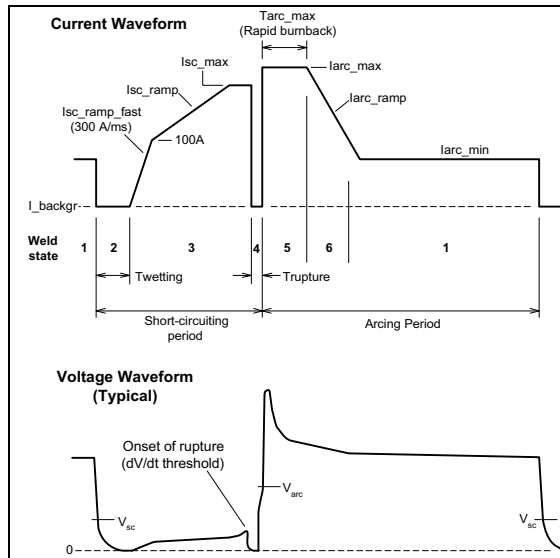


Figure 5 Open loop control waveforms

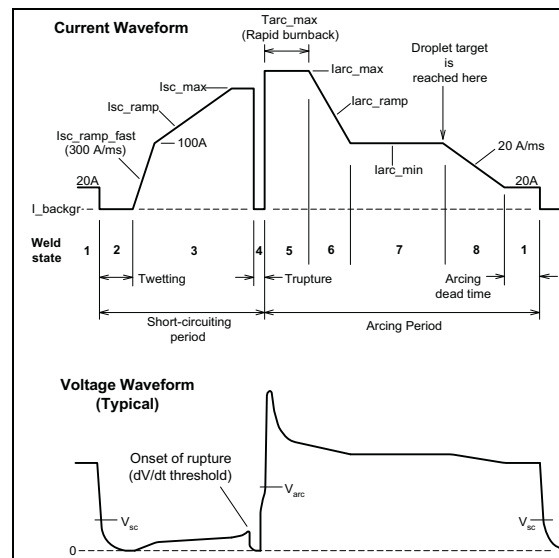


Figure 6 Closed loop control waveforms

PRACTICAL IMPLEMENTATION OF DROPLET SIZE ESTIMATION

The practical implementation of the electrode melting rate model described in equations 1 and 2 poses several problems. Firstly, the calculation of the action $W(t)$ in equation 2 requires the value of the CTWD. In an automated application with a fixed plant (e.g. known electrode type, fixed torch and work leads, fixed mechanical jig), it is feasible to obtain accurate CTWD estimation using through-the-arc sensing techniques, such as that described by Orszagh et al (Ref. 16). A similar technique was developed during the course of this project (Ref. 17) but is not reported in this paper. However, in a manual application, the possible changes in critical plant items (torch and lead lengths, workpiece resistance, work lead clamp connection resistance, electrode composition, and shielding gas mixtures) create possibilities for excessive errors to be introduced in any prospective CTWD estimation algorithm. Errors in the CTWD estimate will cause corresponding errors in the transit time t and action $W(t)$.

Secondly, the relationship between H_L and W as shown in Figure 4 will vary with electrode composition. For a commercial product, it would not be possible to characterise every electrode type available on the market. Use of generic parameters will again lead to estimation errors.

Thirdly, it was found during extensive testing that, even under carefully controlled conditions where all parameters were either known or constant, the model of equation 1 produced errors in the estimated melting rate, integrated over 2.7 seconds of weld time. The errors were consistent with dipping frequency. At low dipping frequencies, the model overestimates the melting rate, while at high frequencies the melting rate is underestimated. The errors were of the order of +/- 10%. This trend suggests that the heat input per unit volume of electrode material H_m varies with welding parameters, and is not the same for all welds. During long arcing times, the final droplet temperature is increased. This conclusion is supported by other research (Refs18-19).

To overcome these problems, a number of assumptions are made so that modelling is simplified.

1. The CTWD is assumed to be either constant (for automated processes), or to remain almost constant during any given transit time τ . This assumes a certain level of skill from a manual operator.
2. The action integral $W(t)$ is assumed to be constant for a stable weld.
3. The heat input per unit volume H_m is assumed to remain constant for a given weld, provided that the welding parameters are not altered. H_m is not necessarily the same for all welds.

The second assumption is not immediately evident, but can be proven experimentally in cases where the weld is at least moderately stable (stability index > 0.5), the CTWD does not vary rapidly, and there are more than five dipping cycles contained within the transit time. Figure 7 shows the action integral evaluated for a typical, stable weld with CTWD=16mm and a wire feed speed of 5.7 m/min. This result indicates that the resistive preheating sustained by an element of electrode approaching the end of the electrode is virtually constant. Although the relationship of H_L to W may not be precisely known for a particular electrode type, it can be deduced that $H_L(t)$ will also remain similarly constant. Equation 1 can therefore be simplified, and integrated during arcing time t_a to evaluate a value which is proportional to the length of electrode ΔL which has been melted.

$$\Delta L = K \int_0^{t_a} i(t) dt \quad (\text{Eq. 4})$$

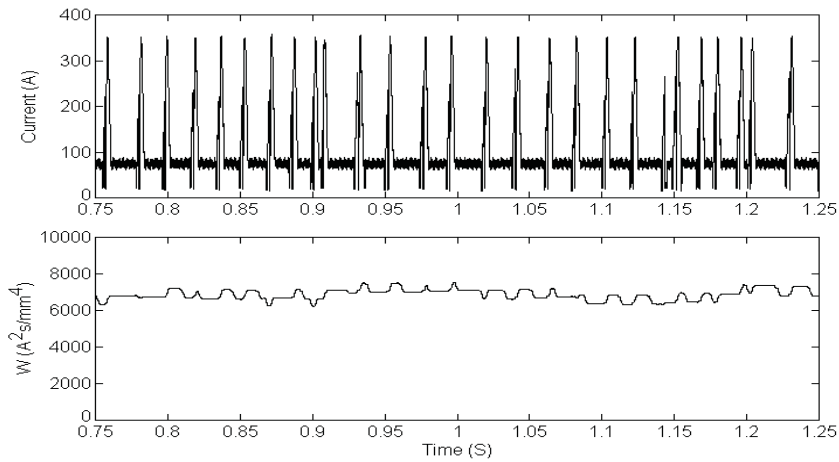


Figure 7 Variation of $W(t)$ during typical weld

The remaining problem is select an appropriate droplet target for the closed loop system. An automatic method of target selection is required, since the proportionality constant K is not known for a given welding condition. A number of methods were devised, and the most effective method consisted of slowly incrementing the target once per weld cycle until a “fault” condition was encountered, at which point the target is reduced by a larger increment back to a safe level. The fault condition is deemed to exist when a short circuit occurs before the current is reduced to the minimum level. This technique maximises droplet size and energy input to the process for a given set of welding parameters, while attempting to minimise initial short-circuiting current (for

spatter reduction) and maintaining a consistent droplet size. Figure 8 shows the variation of droplet size target during a weld.

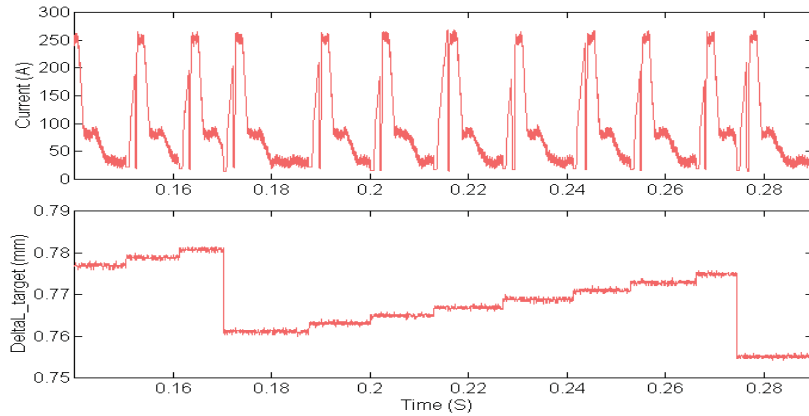


Figure 8 Controlled variation in ΔL_{target} over several welding cycles

VERIFICATION OF DROPLET SIZE ESTIMATION

Having implemented the simplified droplet size estimate of equation 4 in the real time controller, a photographic method was used to verify that the droplets formed at the end of the electrode were of a consistent size. The controlling software was modified so that a fixed droplet size target was used, and the photographic equipment was triggered immediately after the target was reached, at the same time that the arcing current was reduced to the background level. Figure 9 is an example of a photograph taken using a 640x480 pixel digital camera and xenon flash front-lighting.



Figure 9 Typical photograph of droplet

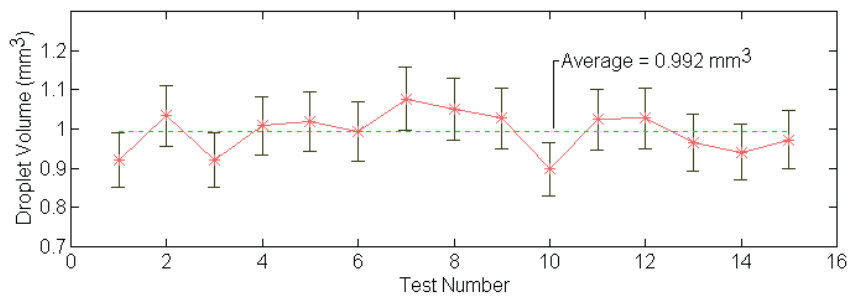


Figure 10 Variation in droplet volume

Fifteen such tests were conducted, and the volume of each droplet was estimated from each photograph. To do this, the droplet was assumed to be axisymmetrical. The image of the droplet was divided into approximately 20 cylindrical “slices”. The scaling was determined from the image of the non-molten electrode, which is known to be 0.9mm in diameter. Figure 10 summarises the estimated droplet volumes. The error bars indicate the range of measurement errors, the greatest of these coming from uncertainties in finding the exact scale of the image and the exact boundary of the droplet. At high magnification, image blurring is significant, and

greater resolution is required for a more accurate result. Also, the assumption of axisymmetry may not be correct, and distortion of the droplet will lead to errors.

Despite the limitations of these tests, the results indicate that the volume of droplets formed by using the simplified estimation technique is sufficiently consistent that variations can be explained by measurement error.

PERFORMANCE EVALUATION OF OPEN LOOP CONTROL

The behaviour of the open loop process was extensively investigated with both Ar-23%CO₂ and CO₂ shielding gases at a wire feed speed of 5.7 m/min, for CTWDs ranging from 8mm to 20mm, and welding speeds of 200mm/min to 400 mm/min. Parameters used to assess the process were stability index, spatter index, fusion area, bead quality, penetration depth, energy input, average droplet size (dipping frequency), mean current, RMS current, and mean voltage. The values and trends in each of these indicate various aspects of process behaviour. The general findings are as follows:

1. The process produces stable, low spatter welds with excellent bead appearance across a very wide range of operating conditions. Good welds can be produced at stability indices down to 0.60, while the more stable welds operate at indices of 0.80 to 0.90.
2. The key parameters of peak arc length, dipping frequency, fusion area and short-circuit transfer characteristics are significantly decoupled. Unlike using CV power sources, the behaviour of the process does not rely on the dynamic characteristics of the power source.
3. The peak arc length is determined by current I_{arc_max} applied early in the arcing period.
4. The fusion area can be adjusted by changing steady state arcing current I_{arc_min} . Fusion can be adjusted over a 2:1 range without altering deposition rate or CTWD. The fusion area was found to be proportional to the energy output of the power source, which is adjusted by I_{arc_min} .
5. The open loop process is able to stably transfer the droplet to the weld pool for a very wide range of droplet sizes. Short-circuit metal transfer is decoupled from arcing considerations because the current during short circuiting is independent of the previous arcing current. As expected from (Ref. 8), metal transfer fails when arcing parameters I_{arc_max} and I_{arc_min} are insufficient for a given wire feed speed. In such conditions, the droplet is too small to form a bridge of sufficient length L_b^* at the next short circuit.
6. The open loop process can produce stable welds with very good bead shapes without the need to synchronise dipping frequency to weld pool oscillation frequency. This is possible because the process is current controlled. The instantaneous welding current is determined by the controller, and does not rely on the complex interaction of a CV power source's dynamic characteristics and the arcing voltage. The dependence on weld pool oscillations is minimised.
7. Truly spatterless welds can be produced under some conditions, and welds with very low spatter levels are produced under most conditions. Spatter produced at the rupture of the short circuit has been virtually eliminated. The main spatter production mechanism is ball repulsion spatter, produced at the start of the short circuit. Generally, as I_{arc_min} is increased, spatter levels rise. However, high spatter can also be produced at very low values of I_{arc_min} if premature short circuits occur early in the arcing period, when the current is still high. This was found to be caused by large weld pool oscillations. In this respect, the welding process is not entirely insensitive to weld pool oscillation.

For brevity, only the key detailed results for CO₂ shielding gas, 12mm CTWD, and 200 mm/min welding speed are presented in this paper. These are representative results, which are used to benchmark the performance of the closed loop process. Figure 11 shows the stability index (Eq. 3) mapped against arcing current parameters I_{arc_max} and I_{arc_min} . These arcing currents determine final droplet size. Figure 12 shows variation in spatter index, which is 10 for a spatterless weld and 0 for a weld with high spatter. From these figures, an optimum operating “ridge” exists for an I_{arc_max} value of 275A. This is the operating condition used to assess the performance of the closed loop droplet size control.

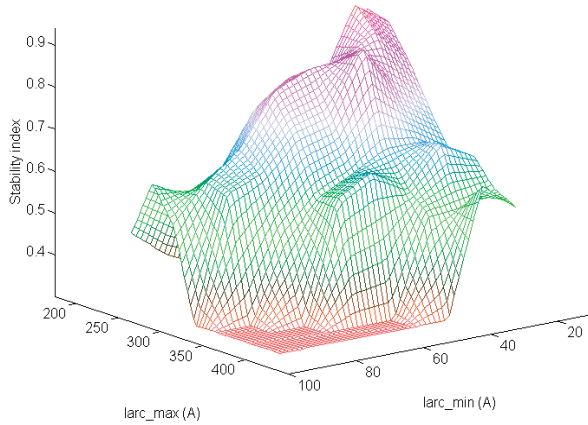


Figure 11 Stability vs I_{arc_max} & I_{arc_min}

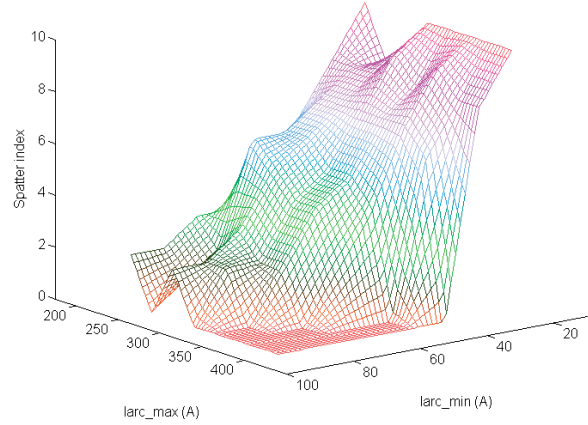


Figure 12 Spatter vs I_{arc_max} & I_{arc_min}

PERFORMANCE EVALUATION OF CLOSED LOOP CONTROL

This section compares the performance of the closed loop droplet size control system to that of the open loop system operating with CO₂ shielding gas, 5.7 m/min wire feed speed, 200mm/min welding speed, 12mm CTWD, and I_{arc_max} value of 275A. In these comparative tests, the value of current I_{arc_min} was varied from 20A to 130A. Above this value, spatter levels became unacceptably high. Figures 13 and 14 show the variations in stability and spatter indices for the two systems.

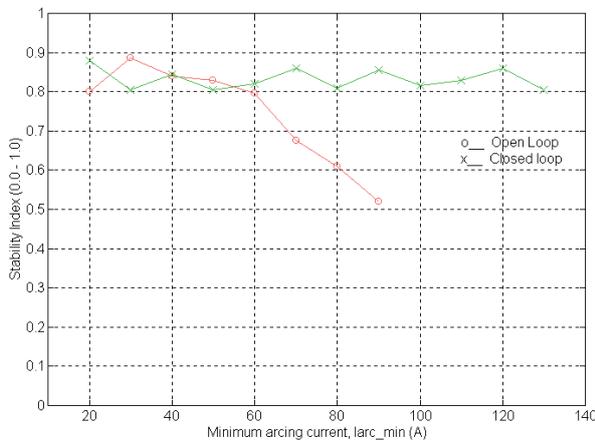


Figure 13 Stability index vs I_{arc_min}

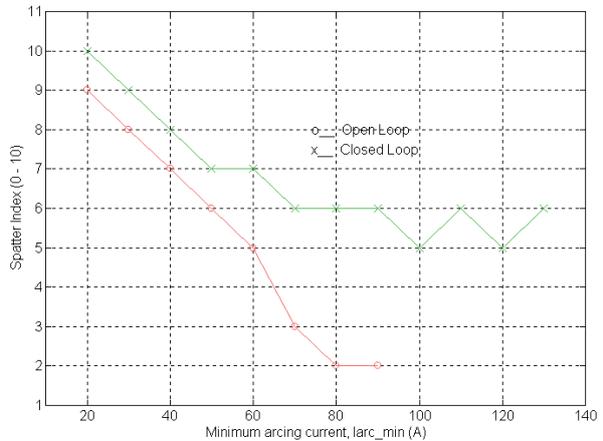


Figure 14 Spatter index vs I_{arc_min}

For a given value of I_{arc_min} , stability is increased and spatter is reduced by the closed loop system. Since the closed loop system is designed to produce short circuits at reduced current (i.e. 20A), it was somewhat surprising that the spatter index was not maintained above 8 throughout the test range. Close inspection of the current and voltage waveforms revealed that “premature” short circuits would infrequently occur early in the arcing period, before the current is reduced to 20A. Figure 15 shows such an event occurring at $t=0.16$ seconds. In this particular recording of 1.0 second duration and 74 short circuiting events, only one such premature short occurs at the nominal value of I_{arc_min} (120A in this case). However, it generates sufficiently high spatter to offset the reduction of spatter in the other 73 weld cycles. These premature short circuits are caused by large weld pool oscillations. Although the closed loop process can produce good weld beads in the presence of such oscillations, spatter cannot be totally suppressed. Depending on the welding conditions, the magnitude of pool oscillations can be minimal. For example, when using Ar-23%CO₂ shielding gas at a welding speed of 200 mm/min and a 16mm CTWD, completely spatterless welds were produced from I_{arc_min} values of 30A to 150A.

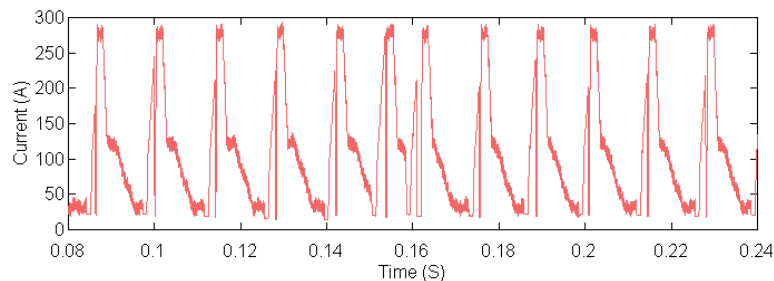


Figure 15 Current waveform at $I_{arc_min}=120A$ showing premature short circuit

The closed loop system produces moderately high stability indices (0.80 to 0.9) across the operating range of I_{arc_min} , but does not improve on the best figures produced by the open loop system. A number of factors are responsible for this. Firstly, the simplified melting rate estimation method is prone to errors. For example, the electrode preheating represented by $W(t)$ is not precisely constant. Also, the electrode stickout length is not constant, but changes by 1.5 to 3mm during the arcing period, albeit in a reasonably consistent manner for each period due to the repeatable current waveform. Secondly, the closed loop control uses a droplet size target which is altered automatically during a weld to find the best operating condition. This implies small changes in the size of the droplets being produced, hence variations in the theoretical weld cycle duration even under zero error conditions. Thirdly, and perhaps most significantly, even small weld pool oscillations will have noticeable effects on the duration of the arcing period even under zero error conditions. For example, at a wire feed speed of 5.7 m/min, a 0.2mm increase in the height of the weld pool surface will cause the short circuit to occur 2.1 milliseconds sooner than if the pool surface did not move. If the average dipping frequency is 70Hz, the change in arcing time is almost 15% of the total weld cycle time. Although simple, these calculations demonstrate how very small weld pool oscillations make high stability indices (greater than 0.90) difficult to achieve across a wide operating range, unless a control scheme is used specifically to reduce weld pool oscillation.

Another important factor which must be taken into account when assessing the overall performance of the closed loop process is the amount of fusion area produced for a given I_{arc_min} setting. Figures 16 and 17 compare the stability and spatter indices produced by open and closed loop processes for comparable fusion areas. These show that there are only marginal

improvements in stability and spatter at higher fusion areas for the closed loop process. The ability for the closed loop process to produce high fusion is hampered by the fact that the current must be reduced at the end of the arcing period, causing a significant reduction in the energy input to the weld. Combined with the infrequent occurrences of premature short circuits which inadvertently produce spatter, the closed loop process does not universally deliver the benefits that are promised by its design. As mentioned previously, the advantage of zero spatter across the entire range of I_{arc_min} values was delivered using Ar-23%CO₂ shielding gas at a welding speed of 200 mm/min and a 16mm CTWD, where the weld pool remains relatively quiescent.

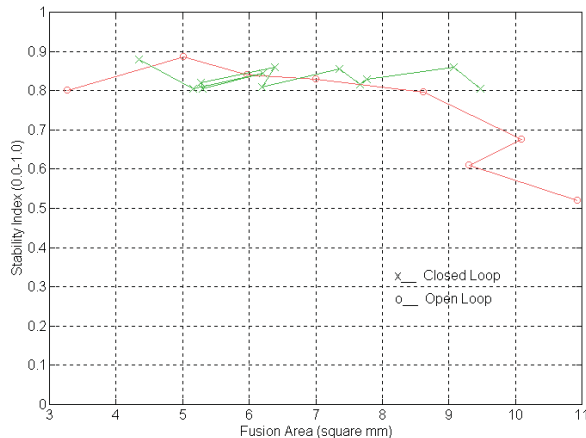


Figure 16 Stability index vs Fusion area

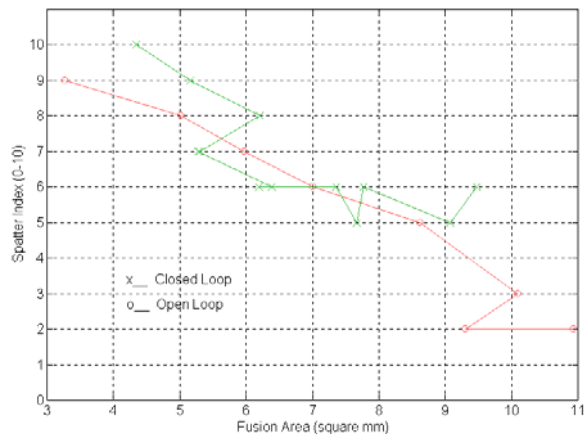


Figure 17 Spatter index vs Fusion area

From results of the tests, two further conclusions can be drawn. Firstly, the value of the stability index is not as critical for the current-controlled process as it is for the constant-voltage (CV) process. Stable welds with very good bead appearance can be produced by the current-controlled process with stability indices as low as 0.60. For the CV process, bead quality suffers noticeably for stability indices below 0.80. The results of the tests have indicated that improvement of stability index above 0.90 is difficult, and the practical benefits are not expected to be significant. Secondly, it has been shown that the single remaining spatter-producing mechanism in the current-controlled processes used here is ball-repulsion generated at the start of the short circuit. If the arcing current can be reduced to a suitably low value (20A) immediately prior to the short circuit, then spatter can be totally eliminated with negligible loss of fusion area.

CONCLUSION

A closed loop droplet size control system has been implemented in a real-time welding controller and applied to a controlled current waveform short-circuit GMAW process. The problems of practical, commercial implementation have been addressed. These include errors in CTWD estimation, possible lack of detailed melting rate constants for various electrode types, variations in melting rate behaviour due to variable droplet temperature, and automatic selection of the optimum droplet size target for all operating conditions. The performance of the closed loop system has been evaluated, and compared to the open loop process. Both processes exhibit decoupling of key parameters such as arc length, fusion area and short-circuit metal transfer characteristics. Also, both processes do not rely on synchronisation of dipping frequency with weld pool oscillation to produce a stable weld.

The closed loop process can improve stability indices and reduce spatter, but not under all conditions. Improvements are possible if weld pool oscillations are minimal, so that premature short circuits are avoided. Increasing stability indices above 0.90 over a wide operating range is difficult, due to the significant influence of even small weld pool movements on the weld cycle duration. The implementation of the droplet size control inherently reduces the fusion area produced for a given arcing current parameter I_{arc_min} .

It is recommended that future development of the controlled current waveform short-circuit GMAW process should concentrate on devising a method to reliably predict the short-circuiting event to within 1ms. Reducing the arcing current to a low value just before the short circuit will totally eliminate spatter with little loss of fusion area.

ACKNOWLEDGEMENTS

The authors gratefully acknowledge the sponsorship of the Cooperative Research Centre for Welded Structures (CRC-WS) and CIGWELD Australia/Thermadyne U.S.A.

REFERENCES

1. Smith, A. A. 1966. Features of short-circuiting CO₂ arc welding with a duplex power source, British Welding Journal April 1966: pp215-223.
2. Boughton, P.; and MacGregor, G. J. 1974. Control of short circuiting in MIG welding. Welding Research International 4(2): pp31-53.
3. Needham, J. C.; and Boughton, P. 1974. Welding power source. U.S. Patent 3792225
4. Ogasawara, T.; Maruyama, T.; Saito, T.; Sato, M.; and Hida, Y.; 1987. A power source for gas shielded arc welding with new current waveforms. Welding Journal March 1987. pp 57-63.
5. Ogasawara, T.; Maruyama, T.; Sato, M.; Hida, Y.; and Saito, T. 1985. Output control of short circuit welding power source. U.S. Patent 4546234
6. Stava, E. K. 1993 .A new, low spatter arc welding machine. Welding Journal January 1993. pp25-29.
7. Boughton, P.; and Martin, T. 1970. An analysis of short circuit MIG systems. BWRA Members' Report P/44/70.
8. Kiyohara, M.; Okada, T.; and Yamamoto, H. 1973. On the stability of metal transfer in short circuit arc welding and the new control systems. IIW Document 212-276-73
9. Lesnewich, A. 1958. Control of melting rate and metal transfer in gas-shielded metal-arc welding, Parts 1 and 2. Welding Journal August 1958 pp343s-353s, and September 1958 pp 418s-425s.
10. Halmoy, E. 1990. Current-voltage process characteristics in GMAW. IIW Document 212-773-90.
11. Halmoy, E. 1986. Electrode wire heating in terms of welding parameters. Appendix A of The Physics of Welding by J.F. Lancaster. Pergamon Press. ISBN 0-08-034076-81986.
12. Halmoy, E. 1996. Simulation and instabilities in GMAW and SAW. IIW Study Group 212: Physics of Welding September 1996 (Budapest Hungary), IIW Document 212-895-96.

13. Buki, A.; and Gorenshtein, I. M. 1967. The stability and self adjustment of metal deposition with short circuits of the arc gap. Automatic Welding 11(1).
14. Shinoda, T.; Kaneda, H.; and Takeuchi, Y. 1989. An evaluation of short circuiting phenomena in GMA welding. Welding and Metal Fabrication 57(10).
15. Kuszelyko, R. 1979. An objective solution of the welding process stability evaluation. IIW Document XII-F208-79.
16. Orszagh, P.; Kim, Y. C.; and Horikawa, K. 1997. Short-circuiting transient phenomena in GMA/CO₂ welding (I): Through-the-wire sensor for feedback torch height control. Transactions of JWRI 26(1). pp49-67.
17. Cuiuri, D. 2000. Control of the short-circuit gas metal arc welding process using instantaneous current regulation. PhD dissertation. University of Wollongong, N.S.W. Australia.
18. Akulov, A. I.; and Spitsyn, V. V. 1968. Rate of formation and transfer of a drop of electrode metal in CO₂ welding. Svar. Proiz No.12. pp7-12.
19. Hirata, Y.; Onda, M.; Nagaki, H; and Ohji, T. 2000. In-situ measurement of metal drop temperature in GMA short-circuiting welding. 53rd Annual Assembly International Institute of Welding. July 9-14, 2000, (Florence, Italy). IIW Document 212-969-00.